Covalently Grafting Nonmesogenic Moieties onto Polyoxometalate for Fabrication of Thermotropic Liquid-Crystalline Nanomaterials

Chang-Gen Lin, Wei Chen, Solomon Omwoma, and Yu-Fei Song*[a]

[a] *State Key Laboratory of Chemical Resource Engineering, Beijing University of Chemical Technology, Beijing 100029, P. R. China. Fax: (+86) 10-64431832; E-mail: songyufei@hotmail.com, songyf@mail.buct.edu.cn*

Experimental Section

Chemical materials: All the chemical materials were purchased from Alpha Aesar and used as received without further purification. Acetonitrile and chloroform were distilled from CaH_2 prior to use.

$[(C_4H_9)_4N]_4[(SiW_{11}O_{39})O\{Si(CH_2)_3NH_2{\bullet}HCl\}_2]$ (**SiW_{11}-NH_2**) was prepared and fully characterized according to the published procedure.[1]

Measurements: ^{1}H-NMR, ^{13}C-NMR, and ^{29}Si-NMR spectra were obtained on a Bruker AV400 NMR spectrometer at resonance frequency of 400 MHz. Fourier transform infrared (FT-IR) spectra were carried out on a Bruker Vector 22 infrared spectrometer using KBr pellet method. Electrospray ionization mass spectra (ESI-MS) were recorded using a Xevo G2 QT ESI-MS, and all experiments were performed in negative mode using acetonitrile as solvent. Elemental Analyses were completed by using varioEL cube from Elementar Analysensysteme GmbH. Thermogravimetric analysis (TGA) was acquired using a TG/DSC 1/1100 SF from METTLER TOLEDO under nitrogen atmosphere with a heating rate of 10 ^oC min^{-1}. Differential scanning calorimeter (DSC) measurements were conducted on a Perkin-Elmer Thermal Analysis instrument with scanning rate of 10 ^oC min^{-1}. The samples were sealed in aluminum capsules and the atmosphere of holder was sustained under dry nitrogen. The optical textures of the mesophases were observed using a Leica DM 2500P optical polarized microscope with a hot stage calibrated to an accuracy of ±0.1 ^oC (Linkam THMS-600). Small-angle X-ray scattering (SAXS) experiments were carried out on a high-flux SAXS instrument (SAXsess, Anton Paar) equipped with a temperature control unit (Anton Paar TCS300). High-resolution TEM (HR-TEM) images were obtained on a JEM 3010 electron microscope equipped with an energy dispersive X-ray (EDX) detector.

4-Hydroxyazobenzene (5): 5 was synthesized according to published method.[2] Yield: 94 %. ^{1}H-NMR ($CDCl_3$, ppm): δ = 5.34 (s, 1H), 6.97 (d, 2H, J = 8.78 Hz), 7.47 (m, 1H), 7.53 (m, 2H), 7.91 (m, 4H). ^{13}C-NMR ($CDCl_3$, ppm): δ = 158.24, 152.71, 147.21, 130.45, 129.06, 125.00, 122.58, 115.81.

4-Bromooctyloxyazobenzene (4a): 5 (1.98 g, 10 mmol) was added to a solution of 1,8-

dibromooctane (6.0 g, 20 mmol) and K_2CO_3 (4.14 g, 30 mmol) in 150 mL acetone. The reaction mixture was refluxed for 24 hours, and then acetone was evaporated under vacuum. The residue was dissolved in chloroform and filtered. After removing chloroform, the resulting orange solid was purified by column chromatography on silica gel using petroleum ether/acetic ether (2:1, v/v) as eluent. Yield: 68 %. ^{1}H-NMR ($CDCl_3$, ppm): δ = 1.34 (m, 4H), 1.50 (m, 4H), 1.87 (m, 4H), 3.44 (t, 2H, J = 13.66 Hz), 4.07 (t, 2H, J = 13.02 Hz), 7.03 (d, 2H, J = 9.00 Hz), 7.46 (m, 1H), 7.52 (m, 2H), 7.92 (m, 4H). ^{13}C-NMR ($CDCl_3$, ppm): δ = 161.67, 152.81, 146.89, 130.30, 129.02, 124.75, 122.54, 114.70, 68.28, 33.97, 32.78, 29.18, 28.69, 28.10, 25.94.

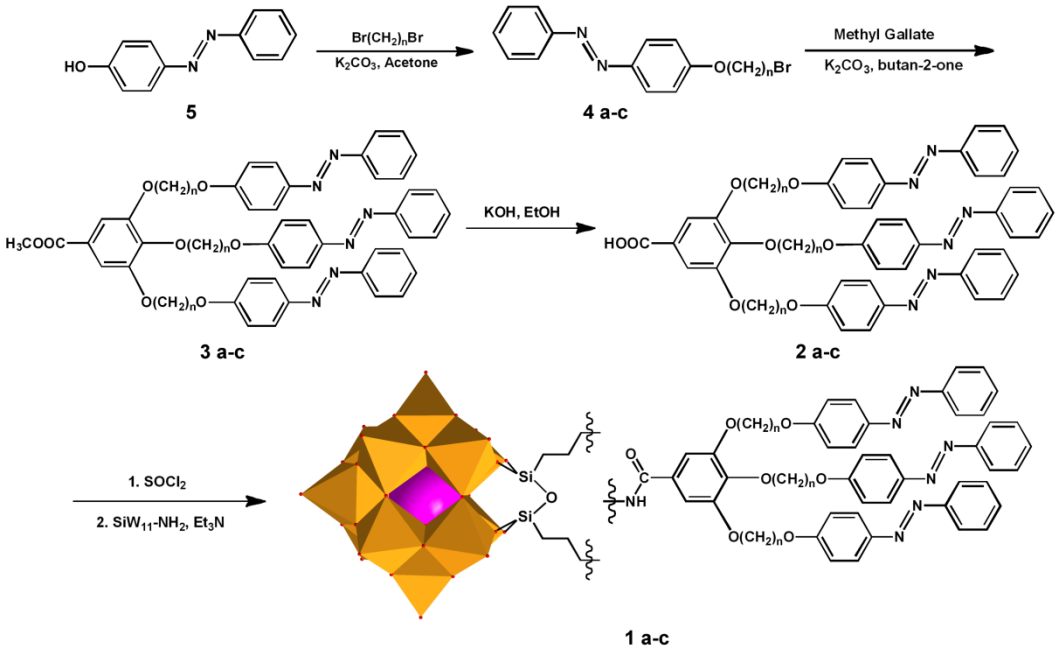

Scheme S1. General syntheses procedure of compounds **1a-c** (a, n = 8; b, n = 10; c, n = 12).

4-Bromodecyloxyazobenzene (4b): A similar procedure was adopted for the synthesis of **4b**. Yield: 75 %. ^{1}H-NMR ($CDCl_3$, ppm): δ = 1.34 (m, 8H), 1.48 (m, 4H), 1.87 (m, 4H), 3.44 (t, 2H, J = 13.72 Hz), 4.07 (t, 2H, J = 13.08 Hz), 7.03 (d, 2H, J = 9.00 Hz), 7.46 (m, 1H), 7.52 (m, 2H), 7.92 (m, 4H). ^{13}C-NMR ($CDCl_3$, ppm): δ = 160.67, 151.77, 145.83, 129.26, 127.98, 123.71, 121.50, 113.66, 67.30, 33.00, 31.79, 28.40, 28.32, 28.29, 28.15, 27.71, 27.13, 24.97.

4-Bromododecyloxyazobenzene (4c): A similar procedure was adopted for the synthesis of **4c**. Yield: 76 %. ^{1}H-NMR ($CDCl_3$, ppm): δ = 1.30 (m, 12H), 1.45 (m, 4H), 1.84 (m, 4H), 3.41 (t, 2H, J = 13.75 Hz), 4.04 (t, 2H, J = 13.11 Hz), 7.00 (d, 2H, J = 9.00 Hz), 7.43 (m, 1H), 7.50 (m, 2H), 7.89 (m, 4H). ^{13}C-NMR ($CDCl_3$, ppm): δ = 161.72, 152.81, 146.87, 130.29, 129.02, 124.74, 122.53, 114.71, 68.37, 34.06, 32.84, 29.53, 29.43, 29.37, 29.19, 28.77, 28.18, 26.01.

Methyl 3,4,5-Tri((8-(4-(phenyldiazenyl)phenoxy)octyl)oxy)benzoate (3a): 4a (1.95 g, 5 mmol) was added to a solution of Methyl Gallate (272 mg, 1.5 mmol), K_2CO_3 (1.05 g, 7.6 mmol), and a catalytic amount of KI in butan-2-one 30 mL. The mixture was stirred at reflux for 36 hours and then butan-2-one was evaporated under vacuum. The residue was washed with petroleum ether and methanol successively for several times. The product was obtained after recrystallization in acetone. Yield: 74 %. ^{1}H-NMR ($CDCl_3$, ppm): δ = 1.41 (m, 12H), 1.50 (m, 12H), 1.79 (m, 12H), 3.89 (s, 3H), 4.02 (m, 12H), 6.98 (m, 6H), 7.25 (s, 2H), 7.42 (m, 3H), 7.49 (m, 6H), 7.88 (m, 12H). ^{13}C-NMR ($CDCl_3$, ppm): δ = 166.93, 161.69, 152.82, 146.88, 142.33, 130.30, 129.03, 124.77, 122.56, 114.70, 108.03, 73.42, 69.11, 68.31, 52.16, 30.33, 29.46, 29.37, 29.30, 29.22, 26.03.

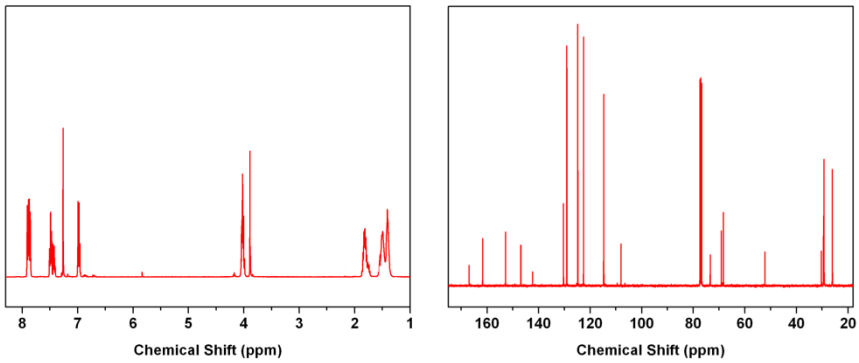

Figure S1. ^{1}H-NMR (left) and ^{13}C-NMR spectra of **3a.**

Methyl 3,4,5-Tri((10-(4-(phenyldiazenyl)phenoxy)decyl)oxy)benzoate (3b): A similar procedure was adopted for the synthesis of **3b**. Yield: 53 %. ^{1}H-NMR ($CDCl_3$, ppm): δ = 1.35 (m, 24H), 1.48 (m, 12H), 1.78 (m, 12H), 3.88 (s, 3H), 4.02 (m, 12H), 6.98 (m, 6H), 7.25 (s, 2H), 7.42 (m, 3H), 7.49 (m, 6H), 7.88 (m, 12H). ^{13}C-NMR ($CDCl_3$, ppm): δ = 166.94, 161.73, 152.82, 146.88, 142.39, 130.29, 129.02, 124.76, 124.75, 122.56, 114.71, 108.04, 73.47, 69.19, 68.26, 52.13, 30.36, 29.67, 29.62, 29.56, 29.48, 29.42, 29.38, 26.09.

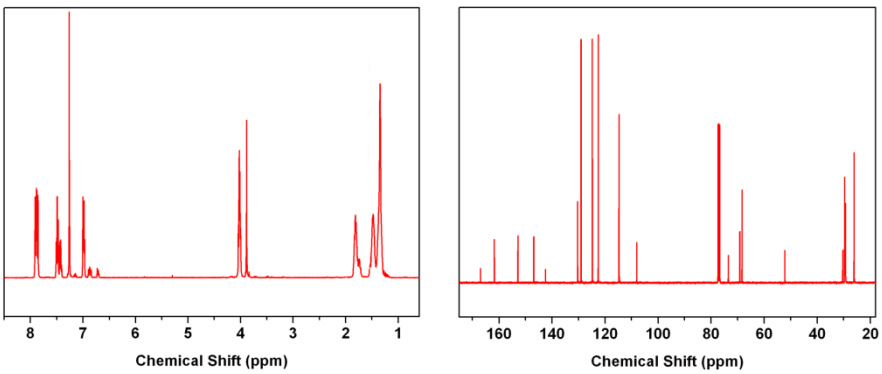

Figure S2. ^{1}H-NMR (left) and ^{13}C-NMR spectra of **3b**.

Methyl 3,4,5-Tri((12-(4-(phenyldiazenyl)phenoxy)dodecyl)oxy)benzoate (3c): A similar procedure was adopted for the synthesis of **3c**. Yield: 72 %. ^{1}H-NMR ($CDCl_3$, ppm): δ = 1.30 (m, 36H), 1.47 (m, 12H), 1.78 (m, 12H), 3.88 (s, 3H), 4.02 (m, 12H), 6.98 (m, 6H), 7.25 (s, 2H), 7.42 (m, 3H), 7.49 (m, 6H), 7.88 (m, 12H). ^{13}C-NMR ($CDCl_3$, ppm): δ = 166.95, 161.73, 152.81, 146.86, 142.36, 130.29, 129.02, 124.75, 122.54, 114.70, 108.00, 73.49, 69.17, 68.37, 52.13, 30.35, 29.71, 29.68, 29.62, 29.43, 29.32, 29.23, 26.08.

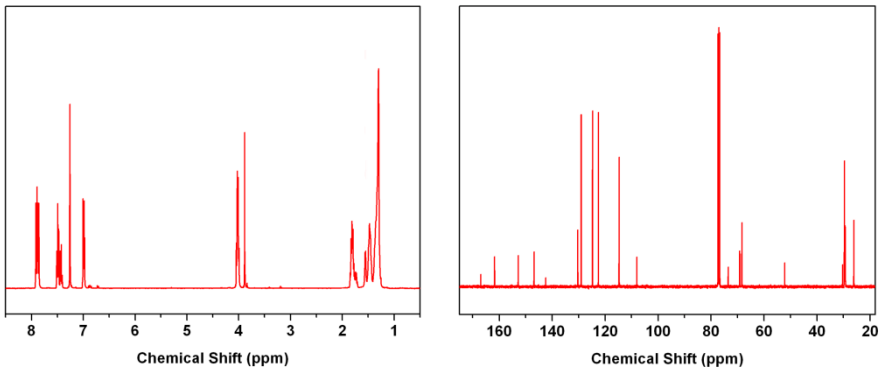

Figure S3. ^{1}H-NMR (left) and ^{13}C-NMR spectra of **3c**.

3,4,5-Tri((8-(4-(phenyldiazenyl)phenoxy)octyl)oxy)benzoic Acid (2a): 3a (500 mg, 0.45 mmol), and KOH (315 mg, 5.6 mmol) were dissolved in THF/EtOH (1:1, v/v) 50 mL and refluxed for 4 h. After evaporating the solvent under reduce pressure, the residue was suspended in 100 mL H_2O and adjusted pH value to 1. The solid compound was collected by filtration and dried in the air. Yield: 92 %. ^{1}H-NMR ($CDCl_3$, ppm): δ = 1.44 (m, 12H), 1.52 (m, 12H), 1.85 (m, 12H), 4.04 (m, 12H), 7.01 (m, 6H), 7.36 (s, 2H), 7.45 (m, 3H), 7.51 (m, 6H), 7.91 (m, 12H). ^{13}C-NMR ($CDCl_3$, ppm): δ = 169.75, 160.65, 151.82, 145.84, 142.06, 129.27, 127.99, 123.73, 122.64, 121.51, 113.66, 107.58, 72.45, 68.11, 67.28, 29.29, 28.41, 28.32, 28.25, 28.22, 28.18, 25.03.

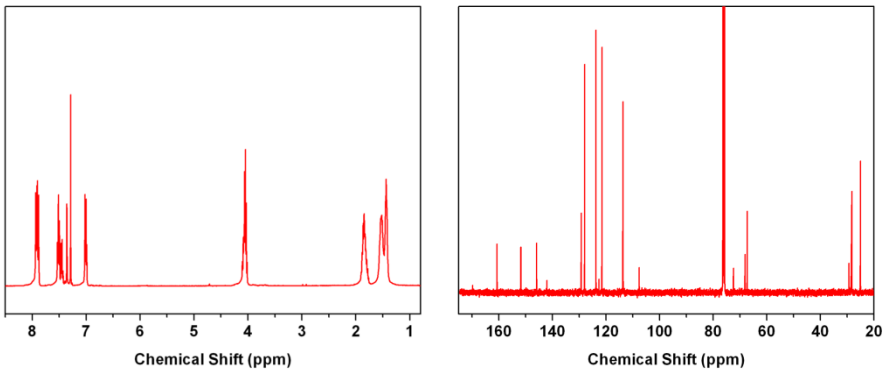

Figure S4. ^{1}H-NMR (left) and ^{13}C-NMR spectra of **2a**.

3,4,5-Tri((10-(4-(phenyldiazenyl)phenoxy)decyl)oxy)benzoic Acid (2b): A similar procedure was adopted for the synthesis of **4b**. Yield: 84 %. ^{1}H-NMR ($CDCl_3$, ppm): δ = 1.34 (m, 24H), 1.48 (m, 12H), 1.80 (m, 12H), 4.03 (m, 12H), 6.98 (m, 6H), 7.31 (s, 2H), 7.42 (m, 3H), 7.49 (m, 6H), 7.88 (m, 12H). ^{13}C-NMR ($CDCl_3$, ppm): δ = 170.75, 161.71, 152.87, 146.86, 143.13, 130.29, 129.02, 124.75, 123.54, 122.66, 114.70, 108.59, 73.53, 69.18, 68.35, 30.35, 29.52, 29.40, 29.36, 29.28, 29.22, 26.04.

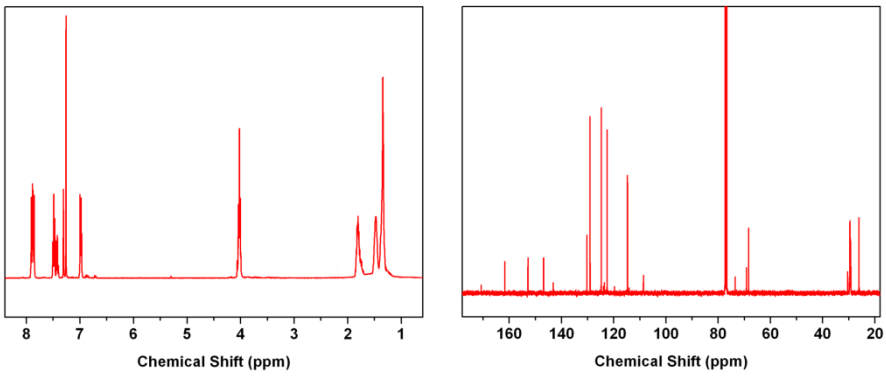

Figure S5. ^{1}H-NMR (left) and ^{13}C-NMR spectra of **2b**.

3,4,5-Tri((12-(4-(phenyldiazenyl)phenoxy)dodecyl)oxy)benzoic Acid (2c): A similar procedure was adopted for the synthesis of **4c**. Yield: 86 %. ^{1}H-NMR ($CDCl_3$, ppm): δ = 1.33 (m, 36H), 1.50 (m, 12H), 1.83 (m, 12H), 4.02 (m, 12H), 7.02 (m, 6H), 7.35 (s, 2H), 7.46 (m, 3H), 7.52 (m, 6H), 7.91 (m, 12H). ^{13}C-NMR ($CDCl_3$, ppm): δ = 169.89, 160.69, 151.77, 145.83, 142.11, 129.26, 127.99, 123.82, 122.51, 121.51, 113.67, 107.55 72.52, 68.17, 67.34, 29.32, 28.67, 28.65, 28.58, 28.43, 28.39, 28.26, 28.19, 25.04.

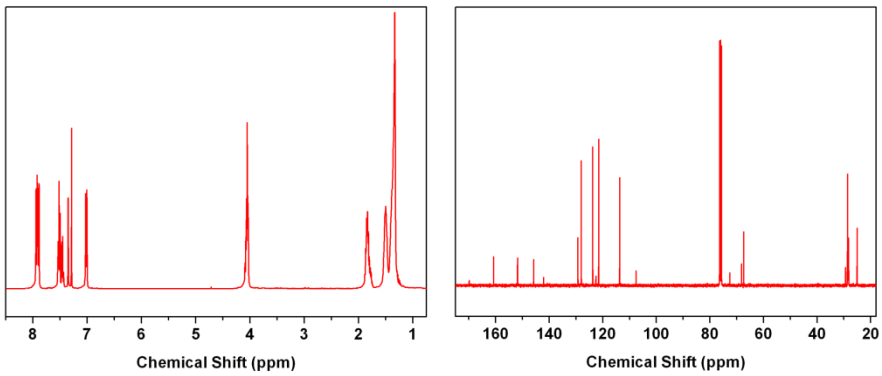

Figure S6. ^{1}H-NMR (left) and ^{13}C-NMR spectra of **2c**.

General Method of preparing 1a-c: 1a-c were prepared according to our previous work.[3] **$[(C_4H_9)_4N]_4[(SiW_{11}O_{39})O\{Si(CH_2)_3NHCOC_6H_2(OC_8H_{16}OC_{12}H_9N_2)_3\}_2]$ (1a)**: Yield: 46 %. ^{1}H-NMR ($CDCl_3$, ppm): δ = 0.90 (m, 4H), 1.00 (t, 48H), 1.32 (m, 24H), 1.51 (m, 56H), 1.68 (m, 32H), 1.82 (m, 24H), 2.02 (m, 4H), 3.30 (m, 36H), 3.63 (m, 4H), 4.03 (m, 24H), 7.00 (m, 12H), 7.43 (m, 6H), 7.50 (m, 12H), 7.89 (m, 24H). ^{13}C-NMR ($CDCl_3$, ppm): δ = 166.65, 161.76, 152.76, 146.79, 144.32, 130.30, 129.03, 124.76, 123.82, 122.54, 114.72, 108.76, 74.31, 68.38, 58.53, 47.69, 30.20, 29.40, 29.22, 26.02, 23.99, 19.72, 13.90, 9.20. ^{29}Si-NMR ($CDCl_3$, ppm): δ = -51.46, -84.95. FT-IR (KBr, cm^{-1}): ν = 3406, 2934, 2871, 1662, 1602, 1582, 1503, 1469, 1414, 1376, 1336, 1299, 1259, 1185, 1143, 1105, 1044, 965, 948, 905, 854, 806, 764, 548, 419. Elemental analysis (%) calcd for $C_{204}H_{312}N_{18}O_{54}Si_3W_{11}$ (5987.24): C 40.89, H 5.21, N 4.21; found: C 40.43, H 4.65, N 4.41.

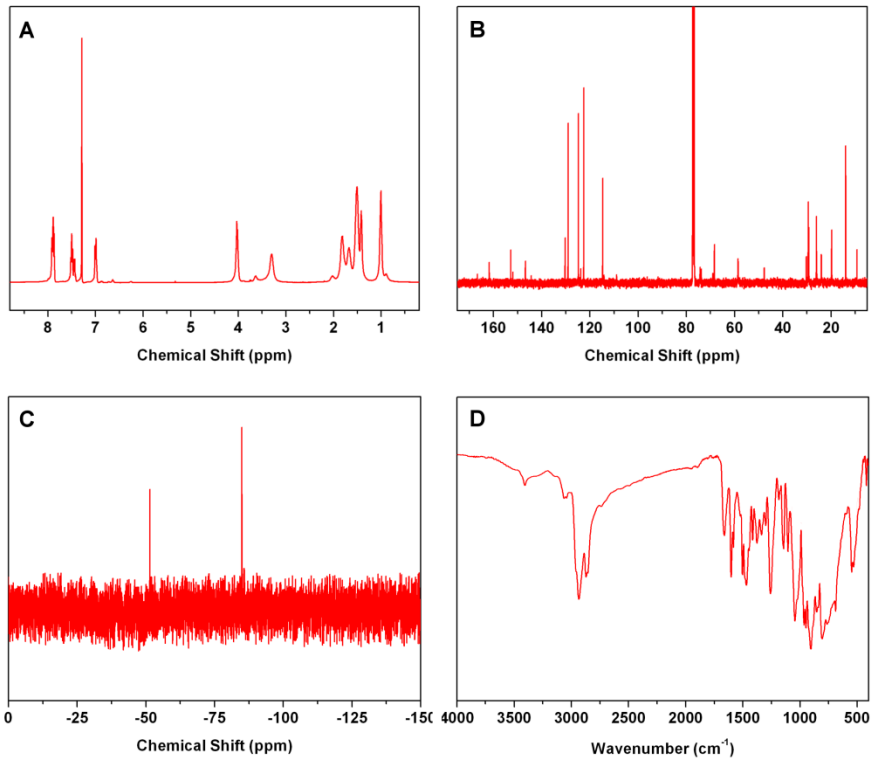

Figure S7. ^{1}H-NMR (A), ^{13}C-NMR (B), ^{29}Si-NMR (C), and FT-IR (D) spectra of **1a**.

$[(C_4H_9)_4N]_4[(SiW_{11}O_{39})O\{Si(CH_2)_3NHCOC_6H_2(OC_{10}H_{20}OC_{12}H_9N_2)_3\}_2]$ (1b): Yield: 52 %. ^{1}H-NMR ($CDCl_3$, ppm): δ = 0.89 (m, 4H), 1.01 (t, 48H), 1.34 (m, 48H), 1.50 (m, 56H), 1.69 (m, 32H), 1.81 (m, 24H), 2.03 (m, 4H), 3.33 (m, 36H), 3.64 (m, 4H), 4.03 (m, 24H), 7.00 (m, 12H), 7.44 (m, 6H), 7.50 (m, 12H), 7.90(m, 24H). ^{13}C-NMR ($CDCl_3$, ppm): δ = 166.61, 161.77, 152.77, 146.80, 143.92, 130.33, 129.04, 124.76, 123.83, 122.55, 114.72, 108.94, 74.13, 58.47, 47.81, 30.24, 29.59, 29.25, 26.08, 24.00, 19.72, 13.94, 9.31. ^{29}Si-NMR ($CDCl_3$, ppm): δ = -52.07, -84.93. FT-IR (KBr, cm^{-1}): ν = 3405, 2930, 2872, 1663, 1601, 1582, 1502, 1469, 1414, 1377, 1337, 1299, 1255, 1184, 1141, 1105, 1044, 964, 948, 905, 853, 806, 766, 549, 419. Elemental analysis (%) calcd for $C_{216}H_{336}N_{18}O_{54}Si_3W_{11}$ (6155.56): C 42.11, H 5.46, N 4.09; found: C 41.85, H 4.93, N 3.88.

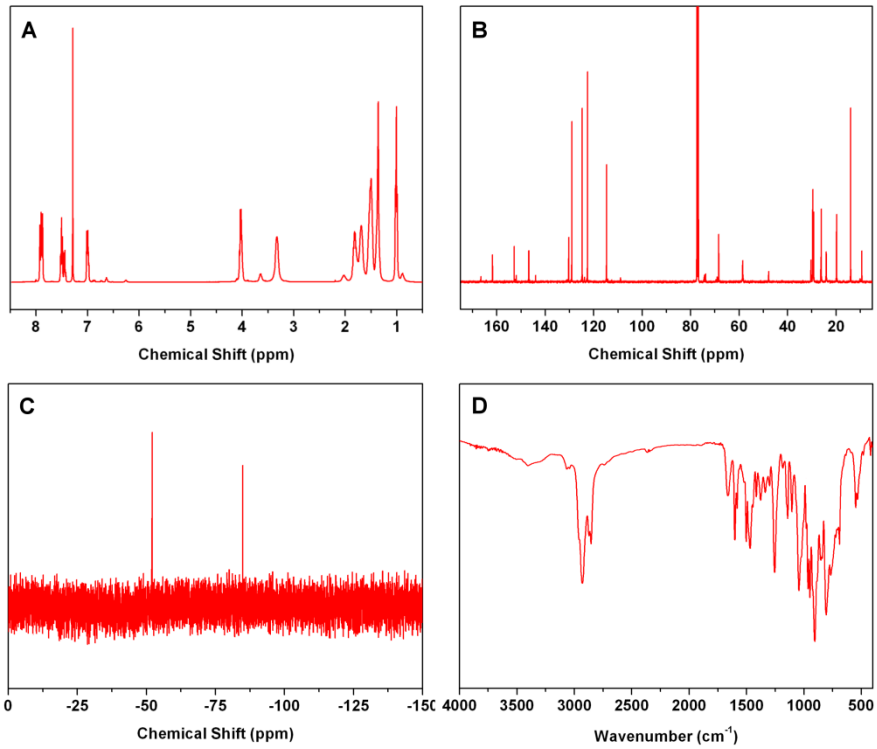

Figure S8. ^{1}H-NMR (A), ^{13}C-NMR (B), ^{29}Si-NMR (C), and FT-IR (D) spectra of **1b**.

$[(C_4H_9)_4N]_4[(SiW_{11}O_{39})O\{Si(CH_2)_3NHCOC_6H_2(OC_{12}H_{24}OC_{12}H_9N_2)_3\}_2]$ (1c): Yield: 62 %. ^{1}H-NMR ($CDCl_3$, ppm): δ = 0.91 (m, 4H), 1.00 (t, 48H), 1.32 (m, 72H), 1.53 (m, 56H), 1.70 (m, 32H), 1.82 (m, 24H), 2.03 (m, 4H), 3.34 (m, 36H), 3.64 (m, 4H), 4.04 (m, 24H), 7.00 (m, 12H), 7.44 (m, 6H), 7.51 (m, 12H), 7.90 (m, 24H). ^{13}C-NMR ($CDCl_3$, ppm): δ = 166.62, 161.75, 152.76, 146.80, 143.90, 130.30, 129.02, 124.74, 123.83, 122.53, 114.70, 108.93, 74.13, 68.39, 58.50, 47.67, 30.23, 29.67, 29.45, 29.22, 26.05, 24.01, 19.72, 13.91, 9.22. ^{29}Si-NMR ($CDCl_3$, ppm): δ = -52.01, -84.92. FT-IR (KBr, cm^{-1}): ν = 3405, 2924, 2852, 1657, 1602, 1582, 1502, 1469, 1415, 1377, 1336, 1256, 1184, 1142, 1105, 1044, 964, 948, 905, 840, 806, 766, 549, 419. Elemental analysis (%) calcd for $C_{228}H_{360}N_{18}O_{54}Si_3W_{11}$ (6323.88): C 43.26, H 5.69, N 3.98; found: C 42.66, H 5.76, N 3.92.

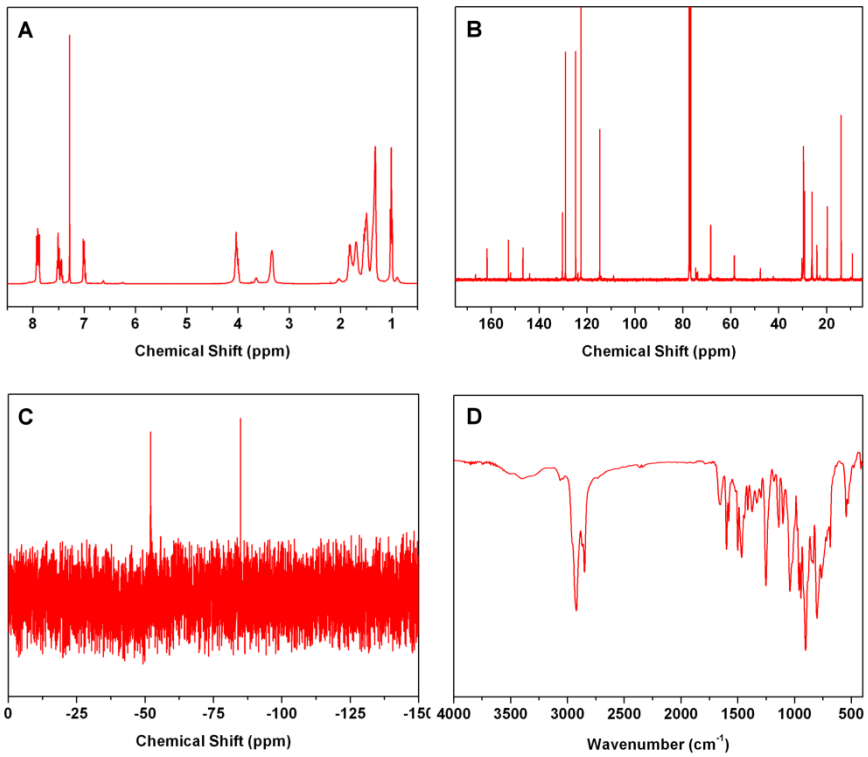

Figure S9. ^{1}H-NMR (A), ^{13}C-NMR (B), ^{29}Si-NMR (C), and FT-IR (D) spectra of **1c**.

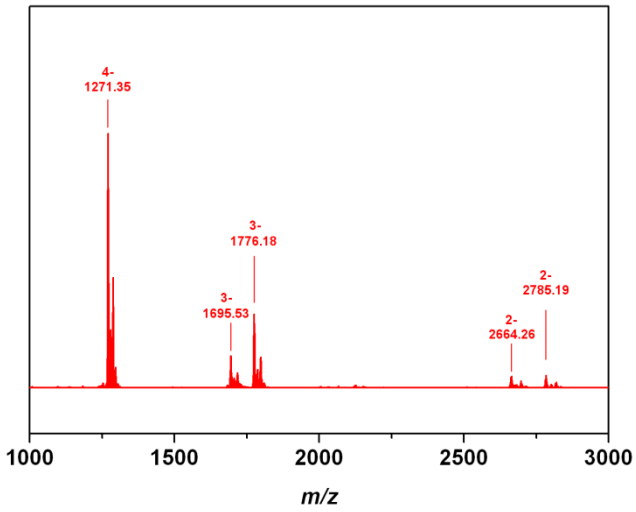

Figure S10. ESI-MS spectrum of **1a**.

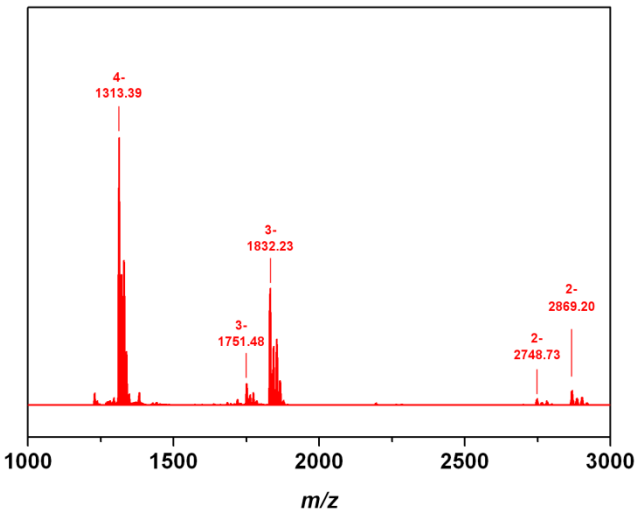

Figure S11. ESI-MS spectrum of **1b**.

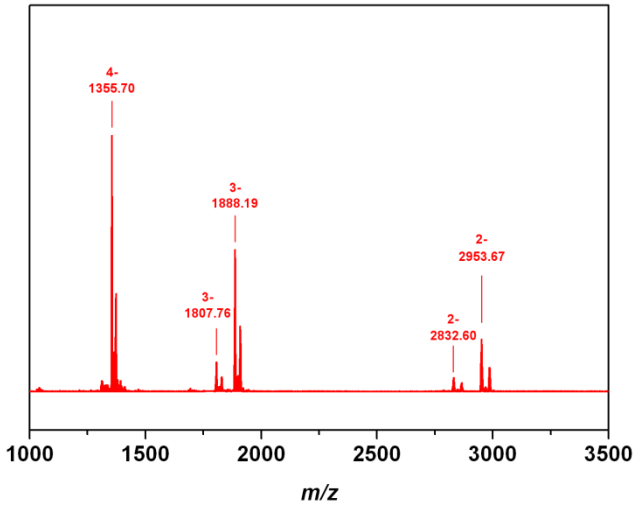

Figure S12. ESI-MS spectrum of **1c**.

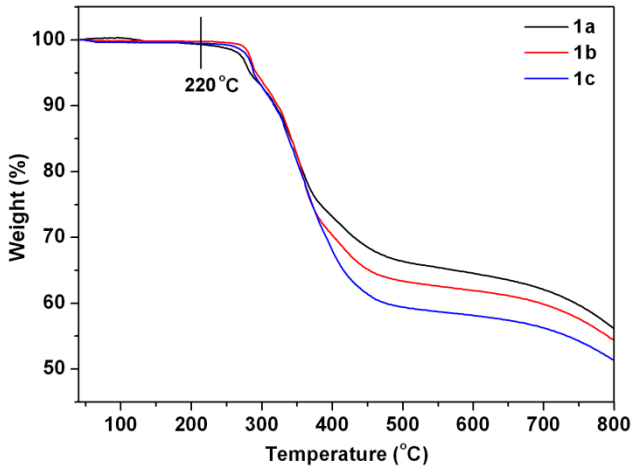

Figure S13. TGA curves of **1a-c** in nitrogen atmosphere at a scanning rate of 10 ºC min^{-1}.

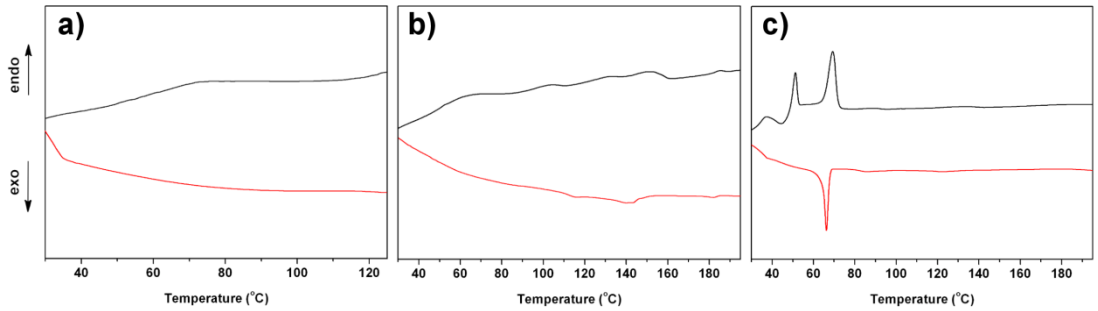

Figure S14. DSC curves of a) **1a**, b) **1b**, and c) **1c** on their first cooling (red) and second heating (black) process.

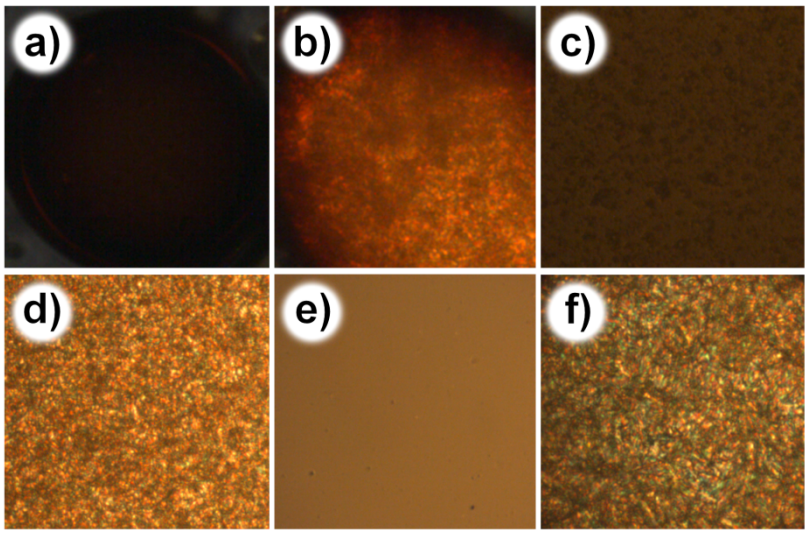

Figure S15. OPM micrographs of (a) **1a** at 200 °C, (b) **1a** at 30 °C, (c) **1b** at 200 °C, (d) **1b** at 30 °C, (e) **1c** at 200 °C, and (f) **1c** at 30 °C during the cooling process (magnification: ×100).

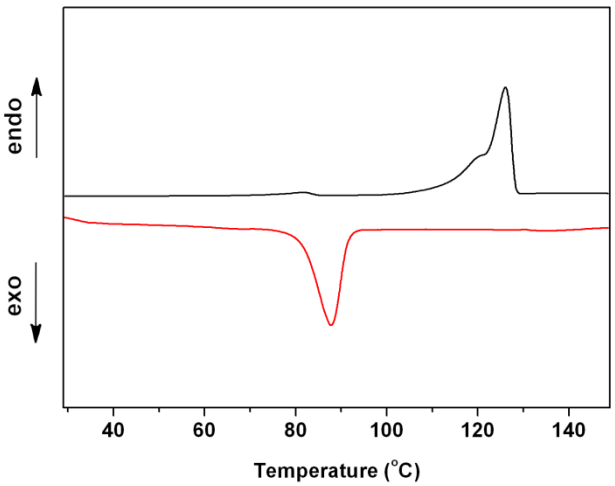

Figure S16. DSC curves of **2c** on its first cooling (red) and second heating (black) process.

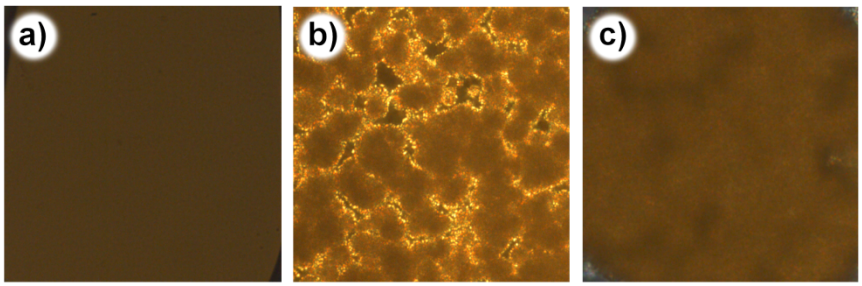

Figure S17. OPM micrographs of **2c** at (a) 150 °C, (b) 90 °C and (c) 30 °C during the cooling process (magnification: ×100).

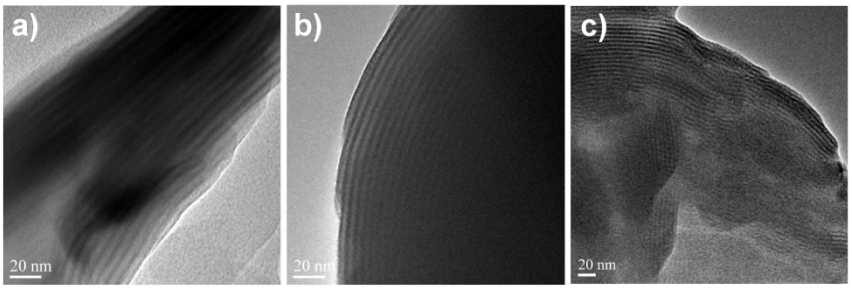

Figure S18. TEM images of a) **1a**, b) **1b**, and c) **1c** after cooling from the isotropic state to room temperature.

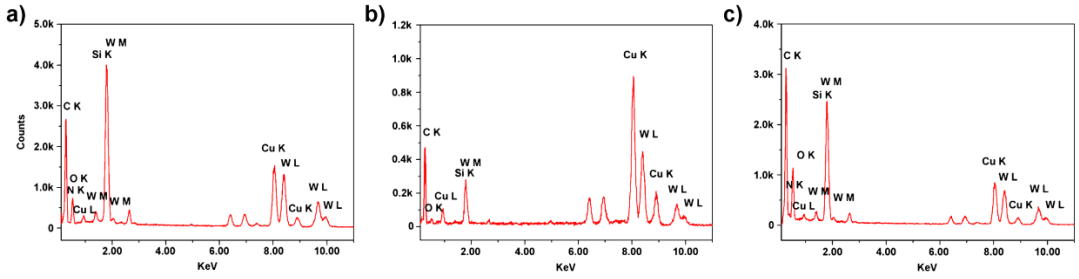

Figure S19. EDX spectra of a) **1a**, b) **1b**, and c) **1c**.

Table S1. The phase transition temperatures, enthalpies and assignments of the phase transition for **1a-c** (G = glass, SmA = smectic A, Iso = isotropic liquid)

Compound	Transition[a]	Temperature/°C	ΔH/kJ mol^{-1}
1a	G-SmA	95.0	—
	SmA-Iso	(193.5)[b]	—
1b	G-SmA_1	113.0	—
	SmA_1-SmA_2	158.7	9.27
	SmA_2- Iso	186.8	1.16
1c	G-SmA_1	70.5	29.80
	SmA_1-SmA_2	100.6	3.78
	SmA_2-SmA_3	168.1	6.06
	SmA_3-Iso	(189.4)	—

[a] Data given on the first cooling process. [b] Data taken from the optical polarized microscopy.

Table S2. Detailed assignment of ESI-MS spectra for compound **1a**

No.	Ion	m/z Calculated	m/z Observed
1	$HCOONa + [(SiW_{11}O_{40})\{Si(CH_2)_3NHCOC_6H_2(OC_8H_{16}OC_{12}H_9N_2)_3\}_2]^{4-}$	1271.35	1271.35
2	$2H_2O + HCOONa + [(SiW_{11}O_{40})\{Si(CH_2)_3NHCOC_6H_2(OC_8H_{16}OC_{12}H_9N_2)_3\}_2]^{4-}$	1280.36	1280.34
3	$4H_2O + HCOONa + [(SiW_{11}O_{40})\{Si(CH_2)_3NHCOC_6H_2(OC_8H_{16}OC_{12}H_9N_2)_3\}_2]^{4-}$	1289.37	1289.33
4	$HCOONa + \{H[(SiW_{11}O_{40})\{Si(CH_2)_3NHCOC_6H_2(OC_8H_{16}OC_{12}H_9N_2)_3\}_2]\}^{3-}$	1695.47	1695.53
5	$2H_2O + HCOONa + \{H[(SiW_{11}O_{40})\{Si(CH_2)_3NHCOC_6H_2(OC_8H_{16}OC_{12}H_9N_2)_3\}_2]\}^{3-}$	1707.48	1707.54
6	$4H_2O + HCOONa + \{H[(SiW_{11}O_{40})\{Si(CH_2)_3NHCOC_6H_2(OC_8H_{16}OC_{12}H_9N_2)_3\}_2]\}^{3-}$	1719.49	1719.52
7	$HCOONa + \{(TBA)[(SiW_{11}O_{40})\{Si(CH_2)_3NHCOC_6H_2(OC_8H_{16}OC_{12}H_9N_2)_3\}_2]\}^{3-}$	1776.29	1776.18
8	$2H_2O + HCOONa + \{(TBA)[(SiW_{11}O_{40})\{Si(CH_2)_3NHCOC_6H_2(OC_8H_{16}OC_{12}H_9N_2)_3\}_2]\}^{3-}$	1788.30	1788.17
9	$4H_2O + HCOONa + \{(TBA)[(SiW_{11}O_{40})\{Si(CH_2)_3NHCOC_6H_2(OC_8H_{16}OC_{12}H_9N_2)_3\}_2]\}^{3-}$	1800.31	1800.14
10	$HCOONa + \{(TBA)H[(SiW_{11}O_{40})\{Si(CH_2)_3NHCOC_6H_2(OC_8H_{16}OC_{12}H_9N_2)_3\}_2]\}^{2-}$	2664.43	2664.26
11	$2H_2O + HCOONa + \{(TBA)H[(SiW_{11}O_{40})\{Si(CH_2)_3NHCOC_6H_2(OC_8H_{16}OC_{12}H_9N_2)_3\}_2]\}^{2-}$	2682.45	2682.24
12	$4H_2O + HCOONa + \{(TBA)H[(SiW_{11}O_{40})\{Si(CH_2)_3NHCOC_6H_2(OC_8H_{16}OC_{12}H_9N_2)_3\}_2]\}^{2-}$	2700.46	2700.22
13	$HCOONa + \{(TBA)_2[(SiW_{11}O_{40})\{Si(CH_2)_3NHCOC_6H_2(OC_8H_{16}OC_{12}H_9N_2)_3\}_2]\}^{2-}$	2785.16	2785.19
14	$2H_2O + HCOONa + \{(TBA)_2[(SiW_{11}O_{40})\{Si(CH_2)_3NHCOC_6H_2(OC_8H_{16}OC_{12}H_9N_2)_3\}_2]\}^{2-}$	2803.18	2803.21
15	$4H_2O + HCOONa + \{(TBA)_2[(SiW_{11}O_{40})\{Si(CH_2)_3NHCOC_6H_2(OC_8H_{16}OC_{12}H_9N_2)_3\}_2]\}^{2-}$	2821.20	2821.18

Table S3. Detailed assignment of ESI-MS spectra for compound **1b**

No.	Ion	m/z Calculated	m/z Observed
1	$HCOONa + [(SiW_{11}O_{40})\{Si(CH_2)_3NHCOC_6H_2(OC_{10}H_{20}OC_{12}H_9N_2)_3\}_2]^{4-}$	1313.43	1313.39
2	$2H_2O + HCOONa + [(SiW_{11}O_{40})\{Si(CH_2)_3NHCOC_6H_2(OC_{10}H_{20}OC_{12}H_9N_2)_3\}_2]^{4-}$	1322.44	1322.39
3	$4H_2O + HCOONa + [(SiW_{11}O_{40})\{Si(CH_2)_3NHCOC_6H_2(OC_{10}H_{20}OC_{12}H_9N_2)_3\}_2]^{4-}$	1331.45	1331.38
4	$HCOONa + \{H[(SiW_{11}O_{40})\{Si(CH_2)_3NHCOC_6H_2(OC_{10}H_{20}OC_{12}H_9N_2)_3\}_2]\}^{3-}$	1751.57	1751.48
5	$2H_2O + HCOONa + \{H[(SiW_{11}O_{40})\{Si(CH_2)_3NHCOC_6H_2(OC_{10}H_{20}OC_{12}H_9N_2)_3\}_2]\}^{3-}$	1763.58	1763.47
6	$4H_2O + HCOONa + \{H[(SiW_{11}O_{40})\{Si(CH_2)_3NHCOC_6H_2(OC_{10}H_{20}OC_{12}H_9N_2)_3\}_2]\}^{3-}$	1775.59	1775.49
7	$HCOONa + \{(TBA)[(SiW_{11}O_{40})\{Si(CH_2)_3NHCOC_6H_2(OC_{10}H_{20}OC_{12}H_9N_2)_3\}_2]\}^{3-}$	1832.06	1832.23
8	$2H_2O + HCOONa + \{(TBA)[(SiW_{11}O_{40})\{Si(CH_2)_3NHCOC_6H_2(OC_{10}H_{20}OC_{12}H_9N_2)_3\}_2]\}^{3-}$	1844.07	1844.21
9	$4H_2O + HCOONa + \{(TBA)[(SiW_{11}O_{40})\{Si(CH_2)_3NHCOC_6H_2(OC_{10}H_{20}OC_{12}H_9N_2)_3\}_2]\}^{3-}$	1856.08	1856.20
10	$HCOONa + \{(TBA)H[(SiW_{11}O_{40})\{Si(CH_2)_3NHCOC_6H_2(OC_{10}H_{20}OC_{12}H_9N_2)_3\}_2]\}^{2-}$	2748.59	2748.73
11	$2H_2O + HCOONa + \{(TBA)H[(SiW_{11}O_{40})\{Si(CH_2)_3NHCOC_6H_2(OC_{10}H_{20}OC_{12}H_9N_2)_3\}_2]\}^{2-}$	2766.61	2766.68
12	$4H_2O + HCOONa + \{(TBA)H[(SiW_{11}O_{40})\{Si(CH_2)_3NHCOC_6H_2(OC_{10}H_{20}OC_{12}H_9N_2)_3\}_2]\}^{2-}$	2784.62	2784.63
13	$HCOONa + \{(TBA)_2[(SiW_{11}O_{40})\{Si(CH_2)_3NHCOC_6H_2(OC_{10}H_{20}OC_{12}H_9N_2)_3\}_2]\}^{2-}$	2869.32	2869.20
14	$2H_2O + HCOONa + \{(TBA)_2[(SiW_{11}O_{40})\{Si(CH_2)_3NHCOC_6H_2(OC_{10}H_{20}OC_{12}H_9N_2)_3\}_2]\}^{2-}$	2887.34	2887.24
15	$4H_2O + HCOONa + \{(TBA)_2[(SiW_{11}O_{40})\{Si(CH_2)_3NHCOC_6H_2(OC_{10}H_{20}OC_{12}H_9N_2)_3\}_2]\}^{2-}$	2905.35	2905.20

Table S4. Detailed assignment of ESI-MS spectra for compound **1c**

No.	Ion	m/z Calculated	m/z Observed
1	$HCOONa + [(SiW_{11}O_{40})\{Si(CH_2)_3NHCOC_6H_2(OC_{12}H_{24}OC_{12}H_9N_2)_3\}_2]^{4-}$	1355.51	1355.70
2	$2H_2O + HCOONa + [(SiW_{11}O_{40})\{Si(CH_2)_3NHCOC_6H_2(OC_{12}H_{24}OC_{12}H_9N_2)_3\}_2]^{4-}$	1364.52	1364.69
3	$4H_2O + HCOONa + [(SiW_{11}O_{40})\{Si(CH_2)_3NHCOC_6H_2(OC_{12}H_{24}OC_{12}H_9N_2)_3\}_2]^{4-}$	1373.53	1373.71
4	$HCOONa + \{H[(SiW_{11}O_{40})\{Si(CH_2)_3NHCOC_6H_2(OC_{12}H_{24}OC_{12}H_9N_2)_3\}_2]\}^{3-}$	1807.68	1807.76
5	$2H_2O + HCOONa + \{H[(SiW_{11}O_{40})\{Si(CH_2)_3NHCOC_6H_2(OC_{12}H_{24}OC_{12}H_9N_2)_3\}_2]\}^{3-}$	1819.69	1819.74
6	$4H_2O + HCOONa + \{H[(SiW_{11}O_{40})\{Si(CH_2)_3NHCOC_6H_2(OC_{12}H_{24}OC_{12}H_9N_2)_3\}_2]\}^{3-}$	1831.70	1831.73
7	$HCOONa + \{(TBA)[(SiW_{11}O_{40})\{Si(CH_2)_3NHCOC_6H_2(OC_{12}H_{24}OC_{12}H_9N_2)_3\}_2]\}^{3-}$	1888.17	1888.19
8	$2H_2O + HCOONa + \{(TBA)[(SiW_{11}O_{40})\{Si(CH_2)_3NHCOC_6H_2(OC_{12}H_{24}OC_{12}H_9N_2)_3\}_2]\}^{3-}$	1900.18	1900.18
9	$4H_2O + HCOONa + \{(TBA)[(SiW_{11}O_{40})\{Si(CH_2)_3NHCOC_6H_2(OC_{12}H_{24}OC_{12}H_9N_2)_3\}_2]\}^{3-}$	1912.19	1912.17
10	$HCOONa + \{(TBA)H[(SiW_{11}O_{40})\{Si(CH_2)_3NHCOC_6H_2(OC_{12}H_{24}OC_{12}H_9N_2)_3\}_2]\}^{2-}$	2832.75	2832.60
11	$2H_2O + HCOONa + \{(TBA)H[(SiW_{11}O_{40})\{Si(CH_2)_3NHCOC_6H_2(OC_{12}H_{24}OC_{12}H_9N_2)_3\}_2]\}^{2-}$	2850.77	2850.56
12	$4H_2O + HCOONa + \{(TBA)H[(SiW_{11}O_{40})\{Si(CH_2)_3NHCOC_6H_2(OC_{12}H_{24}OC_{12}H_9N_2)_3\}_2]\}^{2-}$	2868.78	2868.51
13	$HCOONa + \{(TBA)_2[(SiW_{11}O_{40})\{Si(CH_2)_3NHCOC_6H_2(OC_{12}H_{24}OC_{12}H_9N_2)_3\}_2]\}^{2-}$	2953.48	2953.67
14	$2H_2O + HCOONa + \{(TBA)_2[(SiW_{11}O_{40})\{Si(CH_2)_3NHCOC_6H_2(OC_{12}H_{24}OC_{12}H_9N_2)_3\}_2]\}^{2-}$	2971.50	2971.63
15	$4H_2O + HCOONa + \{(TBA)_2[(SiW_{11}O_{40})\{Si(CH_2)_3NHCOC_6H_2(OC_{12}H_{24}OC_{12}H_9N_2)_3\}_2]\}^{2-}$	2989.51	2989.60

Table S5. The interlayer distances ($d_{001} = 2\pi/q_1$) of **1a-c** calculated from SAXS data at different temperatures

Compound	Temperature/^{o}C	Scattering vector q_1/nm^{-1}	Calculated d_{001}/Å
1a	180	1.1553	54.3857
	130	1.1487	54.6982
	70	1.1425	54.9951
	25	1.1224	55.9799
1b	175	1.0898	57.6545
	130	1.0765	58.3668
	70	1.0759	58.3993
	25	1.0633	59.0914
1c	180	1.0301	60.9958
	130	1.0237	61.3772
	70	1.0103	62.1913
	25	1.0104	62.1851

Reference

[1]. Bar-Nahum, H. Cohen, and R. Neumann, *Inorg. Chem*., 2003, **42**, 3677-3684.

[2]. M. Odabaşoğlu, Ç. Albayrak, R. Özkanca, F. Z. Aykan, and P. Lonecke, *J. Mol. Struct.*, 2007, **840**, 71-89.

[3]. W. Chen, D. Ma, J. Yan, T. Boyd, L. Cronin, D.-L. Long, and Y.-F. Song, *ChemPlusChem.*, 2013, **78**, 1226-1229.